J|A|C|S
ARTICLES
Published on Web 03/08/2003

Ab Initio Simulation of Paramagnetic NMR Spectra: the ^{31}P NMR in Oxovanadium Phosphates

Sébastien Petit,*,† Serguei A. Borshch,† and Vincent Robert†,‡

Contribution from the Laboratoire de Chimie, UMR 5532, CNRS-Ecole Normale Supérieure de Lyon, 46, Allée d'Italie, 69364 Lyon Cedex 07, France and Université Claude Bernard Lyon I, 43, Boulevard du 11 Novembre 1918, 69622 Villeurbanne Cedex, France

Received November 7, 2002; E-mail: spetit@catalyse.univ-lyon1.fr

Abstract: A theoretical analysis of the temperature-dependent ^{31}P NMR signals for the ambient pressure vanadyl pyrophosphate AP-$(VO)_2P_2O_7$ and the oxovanadium hemihydrate hydrogenophosphate $VO(HPO_4)\cdot 0.5H_2O$ phases is reported. The *ab initio* calculation of the magnetic exchange parameters and the hyperfine constants gives access to an original *ab initio* simulation of NMR spectra. Such a strategy allows one to clarify the crystallographic nature of the different experimentally studied phases. For the vanadyl pyrophosphate ambient pressure structure, our simulations strongly support the presence of a monoclinic phase. Based on this assumption, hyperfine constants are extracted from the fit of the experimental data. These values are directly compared to the *ab initio* ones.

1. Introduction

Oxovanadium phosphate compounds have attracted much interest in the physical and chemical communities. The chemical importance of these solids stems from their participation as constituents or precursors of the active phase in a highly efficient industrial catalyst used in the synthesis of maleic anhydride from *n*-butane.[1−3] As the nature of the active site has not been clarified so far, a large range of experimental techniques and theoretical approaches has been called for to investigate this intriguing class of compounds.

On the other hand, the analysis of magnetic properties of the oxovanadium(+IV) phosphate compounds has been very much debated in the literature.[4−23] Each vanadium site V(+IV) being in a d^1 electronic configuration has a local spin of $^1/_2$. The richness of exchange pathways between these paramagnetic centers is responsible for a variety of magnetic interactions. For instance, the vanadyl pyrophosphate $(VO)_2P_2O_7$ compound has long been considered as the first example of the antiferromagnetic spin ladder. However, the temperature dependence of the magnetic susceptibility has been accurately fitted not only by the spin ladder model but also by a rather different one, namely a dimer chain model.[6,7] Thus, the challenge for the theoretical chemists was to evaluate the dominating exchange interactions in order to determine the appropriate magnetic scheme.

Recently, we have reported calculations of exchange constants in different oxovanadium phosphates phases on the basis of a combined B3LYP/Broken-symmetry approach.[21,22] Even though the composition and the geometrical characteristics are quite similar from one phase to another, a wide spectrum of magnetic constants has been observed, ranging from strong antiferromagnetic (∼170 K) to rather small ferromagnetic (∼ −40 K).

Moreover, our *ab initio* evaluations of exchange parameters on molecular dimer models suggested the reformulation or the improvement of the existing magnetic interaction schemes.[4−11] The models which were then called into question usually rely on magnetic susceptibility fits. As mentioned before, the use of susceptibility data might not be well-adapted to conclude on one particular magnetic pattern. However, the ^{31}P nuclear

† CNRS-Ecole Normale Supérieure de Lyon.
‡ Université Claude Bernard Lyon I.

(1) Centi, G. *Catal. Today (special issue)* **1993**, *16*, 1.
(2) Trifiro, F.; Centi, G.; Ebner, J. R.; Franchetti, V. M. *Chem. Rev.* **1988**, *88*, 55.
(3) Bordes, E. *Catal. Today* **1987**, *1*, 499.
(4) Johnson, J. W.; Johnston, D. C.; Jacobson, A. J.; Brody, J. F. *J. Am. Chem. Soc.* **1984**, *106*, 8123.
(5) Wrobleski, J. T. *Inorg. Chem.* **1988**, *27*, 946.
(6) Johnston, D. C.; Johnson, J. W.; Goshorn, D. P.; Jacobson, A. J. *Phys. Rev. B* **1987**, *35*, 219.
(7) Barnes, T.; Riera, J. *Phys. Rev. B* **1994**, *50*, 6817.
(8) Villeneuve, G.; Suh, K. S.; Amorós, P.; Casañ-Pastor, N.; Beltrán-Porter, D. *Chem. Mater.* **1992**, *4*, 108.
(9) Tennant, D. A.; Nagler, S. E.; Garrett, A. W.; Barnes, T.; Torardi, C. C. *Phys. Rev. Lett.* **1997**, *78*, 4998.
(10) Kikuchi, J.; Kurata, N.; Motoya, K.; Yamauchi, T.; Ueda, Y. *J. Phys. Soc. Jpn.* **2001**, *70*, 2765.
(11) Beltrán-Porter, D.; Beltrán-Porter, A.; Amorós, P.; Ibañez, R.; Martinez, E.; Le Bail, A.; Ferrey, G.; Villeuneuve, G. *Eur. J. Solid State Inorg. Chem.* **1991**, *28*, 131.
(12) Garrett, A. W.; Nagler, S. E.; Tennant, D. A.; Sales, B. C.; Barnes, T. *Phys. Rev. Lett.* **1997**, *79*, 745.
(13) Uhrig, G. S.; Normand, B. *Phys. Rev. B* **2001**, *63*, 134418.
(14) Johnston, D. C.; Saito, T.; Azuma, M.; Takano, M.; Yamauchi, T.; Ueda, Y. *Phys. Rev. B* **2001**, *64*, 134403.
(15) Yamauchi, T.; Narumi, Y.; Kikuchi, J.; Ueda, Y.; Tatani, K.; Kobayashi, T. C.; Kindo, K.; Motoya, K. *Phys. Rev. Lett.* **1999**, *83*, 3729.
(16) Kikuchi, J.; Aoki, T.; Motoya, K.; Yamauchi, T.; Ueda, Y. *Physica B* **2000**, *284*−*288*, 1481.
(17) Lawson Daku, L. M.; Borshch, S. A.; Robert, V.; Bigot, B. *Chem. Phys. Lett.* **2000**, *330*, 423.
(18) Roca, M.; Amorós, P.; Cano, J.; Marcos, M. D.; Alamo, J.; Beltrán-Porter, A.; Beltrán-Porter, D. *Inorg. Chem.* **1998**, *37*, 3167.
(19) Koo, H. J.; Whangbo, M. H. *Inorg. Chem.* **2000**, *39*, 3599.
(20) Lawson Daku, L. M.; Borshch, S. A.; Robert, V.; Bigot, B. *Phys. Rev. B* **2001**, *63*, 174439.
(21) Petit, S.; Borshch, S. A.; Robert, V. *J. Am. Chem. Soc.* **2002**, *124*, 1744.
(22) Petit, S.; Borshch, S. A.; Robert, V. *J. Solid State Chem.*, in press.
(23) Koo, H. J.; Whangbo, M. H.; VerNooy, P. D.; Torardi, C. C.; Marshall, W. J. *Inorg. Chem.* **2002**, *41*, 4664.

magnetic resonance (NMR) gives access to the local characteristics of the electronic structure. Such an experimental technique appears to be appropriate to evaluate and to compare the reliability of different magnetic extended models.

The interests of the catalytic and magnetic research communities overlap when this particular technique is used to investigate paramagnetic compounds. Since the first spectrum of the catalytic system was obtained,[24] spin−echo mapping techniques for the ^{31}P nucleus have been extensively used. Indeed, the NMR technique allows experimentalists to identify the presence of one oxovanadium phosphate phase in rather complex systems. From previous studies,[25] the resonance of phosphorus nuclei is reached around 0 ppm in diamagnetic phases V(+V). In the presence of V(+IV) or V(+III), the chemical shift can vary in the range of 2000−4500 ppm[24−26] with a strong temperature dependency. Such high values result from the Fermi contact contribution into the hyperfine structure. A generally accepted interpretation lies in the presence of unpaired d electrons on vanadium atoms which polarize the inner s-shell of the phosphorus atoms giving rise to a nonzero spin electronic density on the latter. Different groups have reported temperature-dependent NMR measurements for two oxovanadium phosphates phases, namely the vanadyl pyrophosphate $(VO)_2P_2O_7$[27−30] and the hemihydrate $VO(HPO_4)\cdot 0.5H_2O$.[30,31] One should stress that the NMR and other experimental data on the $(VO)_2P_2O_7$ compound have been debated with respect to the accurate nature of the crystal structure. In the pioneer work, the orthorhombic structure[32] was proposed for the $(VO)_2P_2O_7$ synthesized under ambient pressure (APO phase). Later on, the crystal structure has been revisited and the authors[33] concluded on a monoclinic phase APM including eight different vanadium atoms and not four as in the APO phase. The most recent studies on a monocrystalline sample using both X-ray and neutron diffraction refinements have ruled out the APM phase in favor of the APO one.[23,34,35] It was suggested that AP-$(VO)_2P_2O_7$ can crystallize both in monoclinic and orthorhombic structures, depending on the preparation conditions. Originally, Tuel et al. have reported temperature-dependent NMR between 150 and 300 K without specifying the space group of the studied sample.[27] Later on, ^{31}P NMR data have been reported for the low-temperature range and the analysis was based on the assumption of an APM crystal phase.[29] Both NMR studies agreed on the presence of four temperature-dependent signals. The NMR data for the hemihydrate phase[30,31] revealed a single temperature-dependent chemical signal.

The main issue in the interpretation of NMR spectra of exchange-coupled extended systems lies in the characterization of the compound spin states. Traditional quantum approaches of chemical shifts[36−39] which have been widely presented over the last years are not suitable for paramagnetic species. It is well-known that the interpretation of NMR data of spin-coupled systems falls within a phenomenological Heisenberg Hamiltonian parametrized by exchange interaction constants.[40,41] Such an approach allows one to extract hyperfine coupling constant values which can be directly compared to *ab initio* estimations. Much effort from experimental[11−14] and theoretical groups[18−23] has been put into the determination of the exchange magnetic patterns and magneto-structural correlations in several oxovanadium phosphates compounds. To bridge the gap between NMR data and magnetic model speculations, we have recently investigated the temperature-dependency of chemical signals in the APM phase.[17] Based on both a dimer chain model and a spin ladder one, the analysis of the four temperature-dependent NMR signals has been undertaken for this particular compound. The crystallographic structure we used was a simplified APM phase, whereas the exchange constants had been extracted in previous experimental data. Although we were able to identify four different types of phosphorus atoms associated to combinations of hyperfine constants, this study did not allow us to rule out one of the two magnetic models.

In the present paper, our goal is to look carefully into the NMR spectrum of AP-$(VO)_2P_2O_7$ compounds in order to clarify the nature of the reported phases. Since the APM unit cell consists of eight different phosphorus atoms, one may expect eight temperature-dependent ^{31}P NMR signals. Thus, we first performed *ab initio* calculations of hyperfine constants *A*. The technical details and the calculated values are given in sections 2.3 and 3.1, respectively. The calculations of the spin state energies and spin projections based on the reported exchange constants *J*[21,22] were performed using a local software which has been developed in our group. The model we considered was a double dimer chain one, detailed in section 2.2. Therefore, the combination of the *ab initio A* and *J* values gives access to our knowledge of the first temperature-dependent paramagnetic NMR spectrum simulation (section 3.2). These *ab initio* simulations are extremely useful in the understanding of the intriguing presence of only four signals. In section 3.3, we extract hyperfine coupling constants from the fit of the experimental data which can be directly compared to the *ab initio* evaluations. Within a very similar framework, the analysis of the temperature-dependent NMR signals in the hemihydrate $VO(HPO_4)\cdot 0.5H_2O$ phases is carried out. We believe that the combination of "full" *ab initio* and experimental fit strategies is extremely valuable in the identification of oxovanadium phosphates phases.

2. Methodological Aspect

2.1. Paramagnetic Chemical Shift. In compounds where several paramagnetic centers are magnetically coupled, NMR data interpretations need special considerations. A featuring effect of the magnetic coupling is the occurrence of a manifold of states characterized by

(24) Li, J.; Lashier, M. E.; Schrader, G. L.; Gerstein, B. B. *Appl. Catal.* **1991**, *73*, 83.
(25) Vedrine, J. C.; Millet, J. M. M.; Volta, J. C. *Faraday Discuss. Chem. Soc.* **1989**, *87*, 207.
(26) Sananes, M. T.; Tuel, A.; Volta, J. C. *J. Catal.* **1994**, *145*, 251.
(27) Sananes, M. T.; Tuel, A. *J. Chem. Soc., Chem. Commun.* **1995**, *13*, 1323.
(28) Tuel, A.; Sananes-Schulz, M. T.; Volta, J. C. *Catal. Today* **1997**, *37*, 59.
(29) Kikuchi, J.; Motoya, K.; Yamauchi, T.; Ueda, Y. *Phys. Rev. B* **1999**, *60*, 6731.
(30) Sananes, M. T.; Tuel, A. *Solid State Nucl. Magn. Reson.* **1996**, *6*, 157.
(31) Furukawa, Y.; Iwai, A.; Kumagai, K. Yakubovsky, A. *J. Phys. Soc. Jpn.* **1996**, *65*, 2393.
(32) Gorbunova, Y. E.; Linde, S. A. *Sov. Phys. Dokl.* **1979**, *24*, 138.
(33) Nguyen, P. T.; Hoffman, R. D.; Sleight, A. W. *Mater. Res. Bull.* **1995**, *30*, 1055.
(34) Hiroi, Z.; Azuma, M.; Fujishiro, Y.; Saito, T.; Takano, M.; Izumi, F.; Kamiyama, T.; Ikeda, T. *J. Solid State Chem.* **1999**, *146*, 369.
(35) Geupel, S.; Pilz, K.; Van Smaalen, S.; Büllesfeld, F.; Prokofiev, A.; Assmus, W. *Acta Crystallogr., Sect. C* **2002**, *58*, i9.
(36) Ramsey, N. F. *Phys. Rev.* **1950**, *78*, 699.
(37) Ramsey, N. F. *Phys. Rev.* **1952**, *86*, 243.
(38) Robert, V.; Petit, S.; Borshch, S. A.; Bigot, B. *J. Phys. Chem. A* **2000**, *104*, 4586.
(39) Malkin, V. G.; Malkina, O. L.; Salahub, D. R. *J. Am. Chem. Soc.* **1995**, *117*, 3294.
(40) Mouesca, J. M.; Noodleman, L.; Case, D. A.; Lamotte, B. *Inorg. Chem.* **1995**, *34*, 4347.
(41) Bertini, I.; Luchinat, C. *Coord. Chem. Rev.* **1996**, *150*, 1.

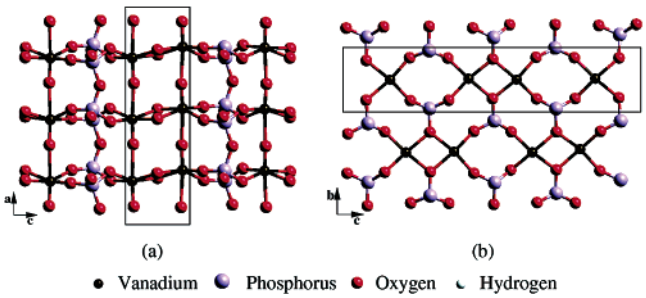

Figure 1. (a) $(VO)_2P_2O_7$ spin ladder structure along the **a** direction in the APO phase. (b) Alternating dimer chain along the **b** direction. The rectangles show the constitutive dimeric units.

different total electronic spins S, populated according to Boltzman's law. Their energies E_n and eigenfunctions $|S_n\rangle$ are given by the diagonalization within each S-manifold of a phenomenological Heisenberg−Dirac−Van Vleck spin Hamiltonian (HDVV):

$$H = \sum_{\langle k,l \rangle} J_{kl} \mathbf{s_k} \cdot \mathbf{s_l} \tag{1}$$

where $\mathbf{s_k}$ and $\mathbf{s_l}$ are the electronic spin operators at sites k and l. This Hamiltonian can be parametrized by the *ab initio* evaluation of the J_{kl} exchange constants.

As soon as the electronic spin density of a given nucleus is polarized by one paramagnetic center M_i, the contribution of the hyperfine interaction to the observed NMR chemical shift reads[41]

$$\delta_{M_i,\mathrm{para}}(T) = \frac{g\mu_B}{g_N\mu_N}\frac{A_{M_i}}{3k_BT}\frac{\sum_S\sum_n K_{M_i}(n)S(S+1)(2S+1)\exp\left(\frac{-E_n}{k_BT}\right)}{\sum_S\sum_n (2S+1)\exp\left(\frac{-E_n}{k_BT}\right)} \tag{2}$$

$$= \frac{g\mu_B}{g_N\mu_N}\frac{A_{M_i}}{3k_BT}F_{M_i}(T) \tag{3}$$

where A_{M_i} is the hyperfine coupling constant that the resonant nucleus (in our case phosphorus atom) would experience if the paramagnetic center M_i (in our case vanadium atom) was not involved in the magnetic coupling. g is the electronic g-factor, and g_N is the nuclear gyromagnetic factor. The summation runs over all energy levels E_n in each S-manifold. The projection coefficients $K_{M_i}(n)$ are given by

$$K_{M_i}(n) = \frac{\langle S_n|\mathbf{s_i}\cdot\mathbf{S}|S_n\rangle}{\langle S_n|\mathbf{S}\cdot\mathbf{S}|S_n\rangle} \tag{4}$$

where $\mathbf{s_i}$ is the electronic spin operator on center i and $\mathbf{S}$ is the total spin operator.

If the nucleus experiences the magnetic influence of several paramagnetic centers M_i, the contribution of the hyperfine interaction to the NMR chemical shift reads

$$\delta_{\mathrm{para}}(T) = \frac{\mathcal{C}}{T}\sum_i A_{M_i} F_{M_i}(T) \tag{5}$$

with $\mathcal{C} = g\mu_B/(3g_N\mu_N k_B)$.

2.2. Magnetic Exchange Scheme and Calculations of Spin States. The crystallographic structure[34] of APO-$(VO)_2P_2O_7$ suggests a spin ladder system resulting from the stacking of di-μ-oxovanadium dimers D_O along the **a** direction (Figure 1a). However, the alternation of double O−P−O-bridged D_{OPO} and D_O dimers is consistent with a dimer chain picture along the **c** axis (Figure 1b). The crystallographic structure of APM-$(VO)_2P_2O_7$ is very similar to this one. One should note that two

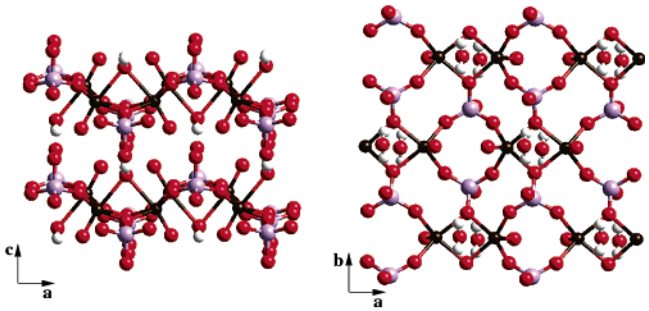

Figure 2. Hemihydrate $VO(HPO_4)\cdot 0.5H_2O$ structure in the (a) **ac** plane and in the (b) **ab** plane.

slightly different chains referred to as A and B are present in the crystal structure. In agreement with very recent experimental fits of inelastic neutron scattering (INS)[12] and light scattering data,[13] our calculations of exchange constants[21] showed that the alternating dimer chain is a valuable starting point for the modeling of $(VO)_2P_2O_7$ APO and APM phases.

The hemihydrate phase $VO(HPO_4)\cdot 0.5H_2O$ is made of dimer chains along the **b** axis organized in a layered structure (see Figure 2). As in the vanadyl pyrophosphate phases, these chains result from the alternation of D_O and D_{OPO} dimers. Even though an isolated dimer picture had been suggested to fit the magnetic susceptibility[11] and the INS experimental data,[9] our recent calculations[22] agreed with NMR measurements,[16] confirming the alternating dimer chain model.

From eqs 2−5, the calculation of the paramagnetic chemical shift relies not only on the knowledge in each S-manifold of the energies E_n but also on the eigenfunctions $|S_n\rangle$. A local software which has been developed in our group allows us to investigate clusters containing up to 16 vanadium sites (spin $^1/_2$). The spin algebra based on the Clebsch−Gordan coefficients gives access to the spin wave functions in terms of the local spin states. One can easily generate the different eigenfunctions of the total spin operator **S** within each S-manifold. Finally, the HDVV Hamiltonian diagonalization in each S-subspace leads to the E_n and $|S_n\rangle$. The ingredients of the magnetic model and the size of the cluster under consideration are two particularly important points. It is clear that the choice of one particular model of magnetic interactions directly controls the number and the values of the exchange parameters.

The HDVV Hamiltonian is parametrized by the reported[21,22] *ab initio* exchange constants. An exact diagonalization for a finite number of interacting centers follows. To properly depict infinite systems, we concentrated on sufficiently large three-dimensional clusters (up to 16 centers). Periodic conditions along the chain's direction were used to achieve a satisfactory description. We must note that it has been shown that 2 × 6 site clusters for the dimer chain model with and without periodic conditions give very similar results.[17] Our criterion for the clusters' sizes along the chain is the convergence of the calculated $F_{M_i}(T)$ functions with respect to the number of magnetic centers in the experimental range of temperature. As soon as the convergence is achieved, a similar number of sites is added along the direction of the dominant interchain coupling.

Within the constraint of the model cluster size, three different magnetic clusters are built for the three reported phases $VO(HPO_4)\cdot 0.5H_2O$, APO-$(VO)_2P_2O_7$, and APM-$(VO)_2P_2O_7$ (Figure 3).

For the hemihydrate compound, an alternating dimer chain has been proposed[21] with two dominating antiferromagnetic exchange constants $J_1 = 122$ K and $J_2 = 77$ K. Since this particular phase exhibits a single vanadium atom per elementary cell, a unique $F^{\mathrm{hemi}}(T)$ function is expected. A series of numerical tests showed that a 6-center cluster is satisfactory. The mapping of the exchange constants in the hemihydrate phase has revealed an interchain ferromagnetic interaction with an

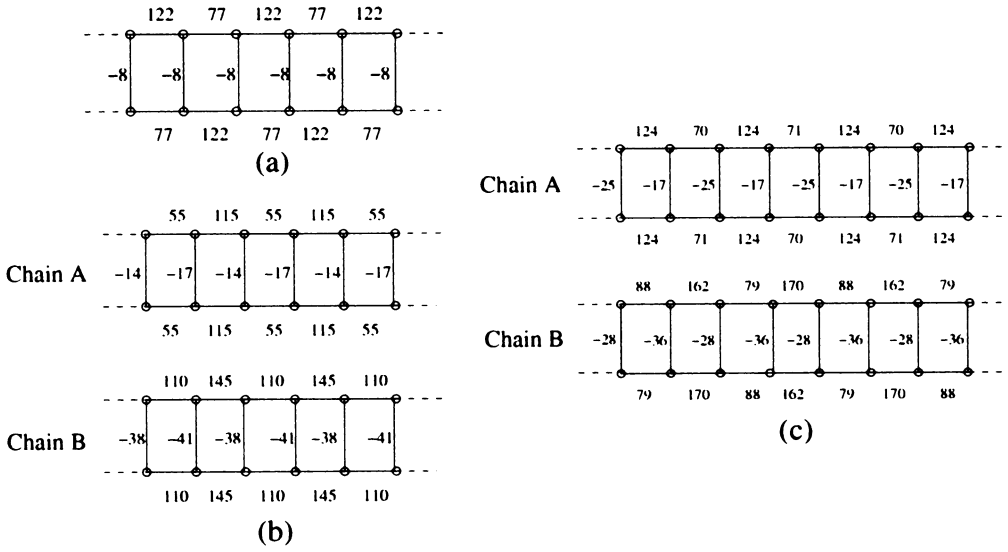

Figure 3. Magnetic clusters used in the F_{M_i} calculations for (a) $VO(HPO_4)\cdot 0.5H_2O$, (b) APO−$(VO)_2P_2O_7$ (four nonequivalent sites), and (c) APM-$(VO)_2P_2O_7$ (eight nonequivalent sites). The numbers on this figure indicate the *ab initio* values[21,22] (in Kelvin) of the exchange constant between two neighboring sites.

exchange constant $J_3 = -8$ K along the **b** direction (see Figure 2b). Therefore, the initial 6-center cluster was extended by adding a second similar cluster coupled through ferromagnetic interactions (Figure 3a). For the APO-$(VO)_2P_2O_7$ phase, one should note that the identification of the model cluster is a bit more problematic. Indeed, too small a cluster size may lead to an unrealistic reduction of the number of $F_{M_i}^{APO}(T)$ functions. The A−B interchain coupling between A and B chains being about a third of the A−A and B−B interchain couplings, two different models (Figure 3b) were extracted separately from the A chains and the B chains, leading to four $F_{M_i}^{APO}(T)$ functions. A very similar strategy was used to build two model clusters for the APM-$(VO)_2P_2O_7$ phase. Each cluster results from the interaction of 16 centers through 6 exchange constants, giving rise to 8 $F_{M_i}^{APM}(T)$ functions (Figure 3c).

2.3. *Ab Initio* Calculations and Experimental Fits of the Hyperfine Constants. The hyperfine coupling constant of a given atom can be written as a function of the electronic spin density on the nucleus $\rho(0)$:

$$A = \frac{8\pi}{3}\cdot g\mu_B\cdot g_N\mu_N\cdot\rho(0) \qquad (6)$$

Therefore, one has to concentrate on the *s*-part of the wave function in the *ab initio* calculation. The electronic spin density can arise from both the presence of unpaired electrons on the atomic site and the polarization effects of neighboring sites. Bertini et al.[41] have suggested that the hyperfine constant in a spin-coupled system can be estimated from monomeric analogues with only one magnetic center. From the crystallographic structures,[33,34,42] we thus considered, for both the AP-$(VO)_2P_2O_7$ and $VO(HPO_4)\cdot 0.5H_2O$ phases, subunits consisting of one vanadium atom V(+IV) in a pseudo-octahedral environment (Figure 4).

Both apical positions are occupied by oxygen atoms, one of them belonging to a water molecule, whereas the second is bounded through a short vanadyl bond V═O (1.61 Å). Each of the four equatorial oxygen atoms belongs to a tetrahedral PO_4 group. By means of protons added along the pre-existing bonds, the oxygen atoms were saturated with a standard O−H distance (0.95 Å). Since the bulk constraints determine the local environment of the polarizing vanadium atom, we did not perform any optimization of the atomic positions of our molecular models.

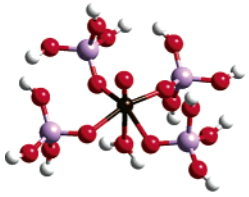

Figure 4. Example of a mononuclear complex used in the *ab initio* calculations of hyperfine constants *A*.

All our *ab initio* calculations of hyperfine coupling constants were performed using the Gaussian98 package.[43] Recent studies indicate that a B3LYP approach is well-adapted to isotropic hyperfine constants calculations.[44−47] This is the one we used in the present study. Since the spin state is doublet, the electronic wave function used to calculate the spin density has been generated within an unrestricted formalism. In this framework, it is known that the resulting wave function does not represent an $\mathbf{S^2}$ eigenstate. However, the calculated expectation value of $\mathbf{S^2}$ is very close to the doublet one 0.75. One main issue in the calculations of hyperfine constants is the determination of an appropriate basis set. Its influence on the hyperfine constants *A* calculations has been investigated for several monomers of the three compounds. It has been previously shown that triple-ζ basis sets are required to reproduce experimentally observed hyperfine constants in mononuclear complexes.[45−47] Thus, all-electron calculations with the basis set 6-311G(d,p) for all atoms were used as references. From our calculations (see the Supporting Information for a comparative study on one particular monomer), the use of a pseudo-potential on the vanadium atom and large basis sets on the resonant phosphorus atoms does not lead to any

(42) Guliants, V. V.; Holmes, S. A.; Benziger, J. B.; Heaney, P.; Yates, D.; Wachs, I. E. *J. Mol. Catal. A* **2001**, *172*, 265.

(43) Frisch, M. J.; Trucks, G. W.; Schlegel, H. B.; Scuseria, G. E.; Robb, M. A.; Cheeseman, J. R.; Zakrzewski, V. G.; Montgomery, J. A.; Stratmann, R. E.; Buran, J. C.; Dapprich, S.; Millam, J. M.; Daniels, A. D.; Kudin, K. N.; Strain, M. C.; Farkas, O.; Tomasi, J.; Barone, V.; Cossi, M.; Cammi, R.; Mennuci, B.; Pomelli, C.; Adamo, C.; Clifford, S.; Ochterski, J.; Peterson, G. A.; Ayala, P. Y.; Cui, Q.; Mokuma, K.; Malick, D. K.; Rabuk, A. D.; Raghavachari, K.; Foresman, J. B.; Cioslowski, J.; Ortiz, J. V.; Stefanov, B. B.; Liu, G.; Liashenko, A.; Piskorz, P.; Komaromi, I.; Gomperts, R.; Martin, R. L.; Fox, D. J.; Keith, T.; Al-Laham, M. A.; Peng, C. Y.; Nanayakkara, A.; Gonzalez, C.; Challacombe, M.; Gill, P. M. W.; Johnson, B. G.; Chen, W.; Wong, M. W.; Andres, J. L.; Head-Gordon, M.; Replogle, E. S.; Pople, J. A. *Gaussian98*, revision A.7; Gaussian, Inc.: Pittsburgh, PA, 1998.

(44) Rega, N.; Cossi, M.; Barone, V. *J. Chem. Phys.* **1996**, *105*, 11060.

(45) Wesolowski, S. S.; Johnson, E. M.; Leininger, M. L.; Crawford, T. D.; Schaefer, H. F. *J. Chem. Phys.* **1998**, *109*, 2694.

(46) Braden, D. A.; Tyler, D. R. *J. Am. Chem. Soc.* **1998**, *120*, 942.

(47) Pauwels, E.; Van Speybroeck, V.; Lahorte, P.; Waroquier, M. *J. Phys. Chem. A* **2001**, *105*, 8794.

significant changes. Variations of less than 5% with respect to the all-electron reference are obtained. One may argue that the inner-core electrons of the vanadium atom do not participate in the polarization of phosphorus *s*-orbitals. In conclusion, the vanadium atom was described by means of the pseudo-potential LANL2, whereas the basis set 6-311G(d,p) was used for all the other atoms.

Finally, in eq 5, one has to select the dominating hyperfine interactions which effectively contribute to the paramagnetic shift. Since the hyperfine interaction on phosphorus atoms results from the polarization of the inner *s*-shell by the spin density on each vanadium site, a careful analysis of the crystal structure is required. As a fair approximation, we may assume that the first nearest-neighbor vanadium atoms are to be included in the electronic spin density polarization of the phosphorus atom. Therefore, the number of nearest neighbors determines the number of hyperfine coupling constants A_{M_i} in eq 5. Let us remind that the number of nonequivalent phosphorus atoms corresponds to the expected number of NMR signals.

In the hemihydrate phase $VO(HPO_4)\cdot 0.5H_2O$, the unique phosphorus atom in the unit cell is surrounded by four vanadium atoms (Figure 2b). Nevertheless, the symmetry of the crystallographic structure reduces the number of hyperfine constants to one A_{OPO} and one A_O. A_{OPO} and A_O are the constants of the hyperfine interactions induced by a vanadium atom through oxygen atoms belonging to O−P−O and μ-oxo bridges, respectively. For this particular compound, the unique temperature-dependent paramagnetic shift reads

$$\delta_{para}(T) = \frac{\mathcal{C}}{T}[2(A_{OPO} + A_O)\cdot F^{hemi}(T)] \quad (7)$$

For the AP-$(VO)_2P_2O_7$, the situation is slightly more complicated since APO and APM phases contain four and eight nonequivalent phosphorus atoms, respectively. Each phosphorus atom is surrounded by four vanadium atoms (Figure 1b). One should note that, in the APO phase, each phosphorus atom is surrounded by the same set of four vanadium atoms (i.e., four $F^{APO}_{M_i}$ functions). However, the contribution of these four paramagnetic centers differs from that of one resonating site to another, leading effectively to four NMR signals. Conversely, in the APM phase eight $F^{APM}_{M_i}$ functions associated to the eight nonequivalent vanadium atoms can be calculated. From the crystallographic structure, we observed that the phosphorus atoms can be gathered in pairs experiencing the fields of the same four vanadium atoms (same $F^{APM}_{M_i}$ functions).

Following this analysis, two different strategies can be considered. One may use the *ab initio* values of the hyperfine constants (see earlier) to evaluate the paramagnetic chemical shift (eq 3). On the other hand, one can extract hyperfine constants from experimental fits to the temperature-dependent NMR signals. In the latter procedure, it should be reminded that the chemical shift of a phosphorus atom *K* involves two contributions, namely the temperature-independent diamagnetic δ^K_{dia} and the previously mentioned paramagnetic one $\delta^K_{para}(T)$. The adjustment was performed by minimizing the function:

$$\mathcal{R} = \frac{1}{N-n}\frac{\sum_K\sum_j[\delta^K_{exp}(T_j) - (\delta^K_{dia} + \delta^K_{para}(T_j))]^2}{\sum_K\sum_j[\delta^K_{exp}(T_j)]^2} \quad (8)$$

where *K* refers to the different NMR signals, *N* is the number of experimental points, and *n* the number of parameters we used. For the AP-$(VO)_2P_2O_7$ compounds, the low-temperature ^{31}P NMR spectrum[29] indicates that the different phosphorus nuclei have very similar diamagnetic shifts (≈ -150 ppm). Therefore, a single parameter for δ_{dia} was optimized for the experimental shifts. For the APM phase of $(VO)_2P_2O_7$, the number of phosphorus atoms is twice the number of NMR signals. Lawson Daku et al.[17] used a simplified model and were able to identify four different phosphorus atoms. However, one may expect the presence of eight different temperature-dependent signals associated to the eight nonequivalent phosphorus atoms. In section 3.2, we will see that the *ab initio* approach turns out to be extremely useful to clarify this particular issue.

Table 1. *Ab Initio* Values of the Hyperfine Constants (MHz) in the APM Phase[33]

phosphorus atom	*A* (MHz)	phosphorus atom	*A* (MHz)
P1	8.00, 9.10, 26.8, 35.4	P5	14.0, 21.5, 27.4, 32.0
P2	4.66, 25.7, 30.0, 31.0	P6	14.8, 22.0, 31.4, 33.9
P3	9.00, 12.1, 30.7, 37,4	P7	8.30, 28.0, 29.8, 33.0
P4	3.44, 24.8, 30.1, 31.0	P8	18.5, 23.1, 31,3 34.9

Table 2. *Ab Initio* Values of the Hyperfine Constants (MHz) in the APO Phase[34]

phosphorus atom	*A* (MHz)
P1	5.85, 9.64, 10.3, 23.5
P2	2.14, 27.4, 28.6, 32.5
P3	9.91, 15.9, 28.4, 43.6
P4	5.03, 20.1, 34.3, 52.6

3. Results and Discussion

3.1. *Ab Initio* Hyperfine Constants Calculations. The calculated hyperfine constants for the APM and APO phases using the 6-311G(d,p) basis set are reported in Table 1 and Table 2.

For the hemihydrate compound $VO(HPO_4)\cdot 0.5H_2O$, the *ab initio* hyperfine constants are $A_{OPO} = 3.34$ MHz and $A_O = 13.5$ MHz. In the case of the AP-$(VO)_2P_2O_7$, the sum of the four hyperfine constants on a given phosphorus is approximately overestimated by a factor 1.5 as compared to the values which have been previously found[17] from experimental fits in the APM phase. This difference is definitely due to the limitations of our mononuclear molecular model for the calculation of hyperfine parameters in extended solids. The variations of the hyperfine constants with respect to the V−P distance are presented in Figure 5a. One immediately sees that there is no monotonic behavior. However, the hyperfine constant can be correlated to some extent to the dihedral angle ϕ specifying the bridging phosphorus atom position with respect to the vanadyl oxygen atom (Figure 5b). Let us concentrate on a particular phosphorus atom of the mononuclear complex (Figure 4) and on the singly highest occupied orbital (SOMO) of the *ab initio A* calculations. The main contribution is the $3d_{xy}$ orbital on the vanadium V_1 atom and the p_x orbital on the equatorial oxygen O_2 atom (Figure 5c). As soon as ϕ reaches zero, the phosphorus s orbitals lie in the nodal region of the oxygen atom p_x orbital, canceling the spin polarization. In the D_O dimers, the ϕ angle values imply the two bridging oxygen atoms are close to 90°, whereas they are almost 0° in the D_{OPO} dimers. Thus, the hyperfine constants are larger in the D_O dimers, a counterintuitive result if one focuses on the V−P distance. It should be noticed that our *ab initio* calculations disagree with previous studies[17,29] suggesting the dominant polarizing effect of D_{OPO} vanadium atoms.

3.2. Simulation of NMR Spectra. The contribution of one specific vanadium site to the paramagnetic shift of a phosphorus atom depends on several ingredients, namely the hyperfine constant and the magnetic exchange constants. In the present paper, the hyperfine constants are explicitly evaluated by means of *ab initio* calculations. On the other hand, the magnetic coupling constants were taken from previous work.[21,22] There-

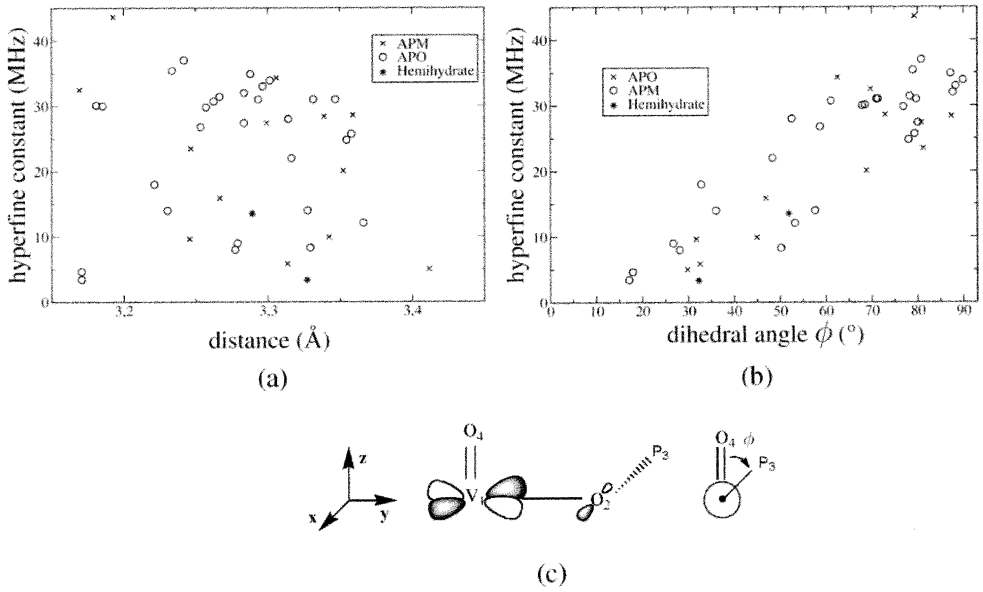

Figure 5. (a) Hyperfine constant variations as a function of V−P distance, (b) hyperfine constant variations as a function of ϕ angle, and (c) schematic representation of ϕ angle.

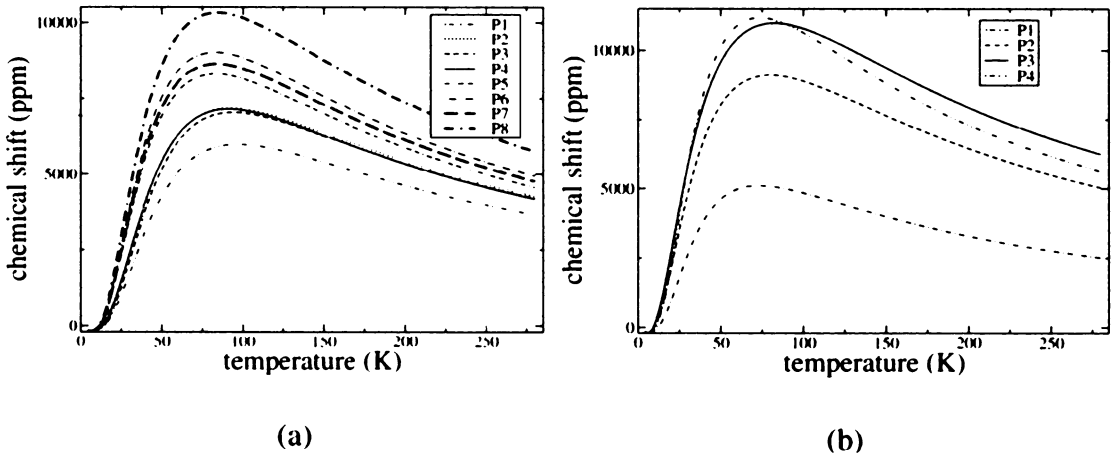

Figure 6. Temperature-dependent ^{31}P NMR simulation: (a) for the APM phase and (b) for the APO phase.[34]

fore, a full *ab initio* simulation of the temperature-dependent paramagnetic part of the chemical shift for the ambient pressure phases of $(VO)_2P_2O_7$ is accessible. We used as a diamagnetic part the experimental value $\delta_{dia} = 150$ ppm in the simulations of the spectra for all phosphorus atoms.

The temperature-dependent ^{31}P NMR spectra for the APM and the APO phases are given in Figure 6. One should note that the NMR shifts are overestimated by a factor ≈ 1.5. Such observation is a reflection of the *ab initio* overestimations of the hyperfine constants. However, these simulations are extremely valuable in the interpretation of the NMR spectra. In particular, the comparison between the experimental data and the *ab initio* simulations of chemical shifts allows one to clarify the actual crystallographic structure of the studied phase. Let us first assume that the ambient pressure phase is monoclinic (APM). Figure 6a shows eight NMR signals, as suggested from the presence of eight nonequivalent phosphorus atoms in the crystal structure. In agreement with experimental observations, the temperature-dependent signals are nonmonotonic curves with a maximum near 85 K (78 K in the NMR experiments). Besides, in the low-temperature regime, the NMR shifts merge into two groups as experimentally observed. The main disagreement with experimental data comes from the number of NMR signals. However, one can gather the simulated lines in four groups according to the values of the NMR chemical shifts. These four groups consist successively of 1, 3, 3, and 1 NMR signals. Around 7000 ppm, the three temperature-dependent shifts are almost perfectly stacked. In the range of 8000 ppm, the maximum splitting between the three signals is ∼350 ppm, that is, ∼3% of the NMR shift. On the other hand, the relative separation between the four experimental signals is ∼15%. Thus, one may assume that the deconvolution with Gaussian functions which has been performed may not allow us to identify the presence of three signals. Finally, from a careful examination of the experimental spectra,[27−29] one can estimate the relative intensities as 1:3:3:1. As the signal intensities for all sites can be reasonably supposed equal, the two central most intense lines may result from the sticking of the three signals. Such an observation supports our *ab initio* description of the APM ^{31}P NMR spectra. Therefore, *ab initio* simulations allow us to settle the apparent discrepancy between the experimental NMR data and the APM phase crystallographic structure. Besides, unambiguous assignments of the NMR shifts to the different phosphorus atoms can be done from our calculations.

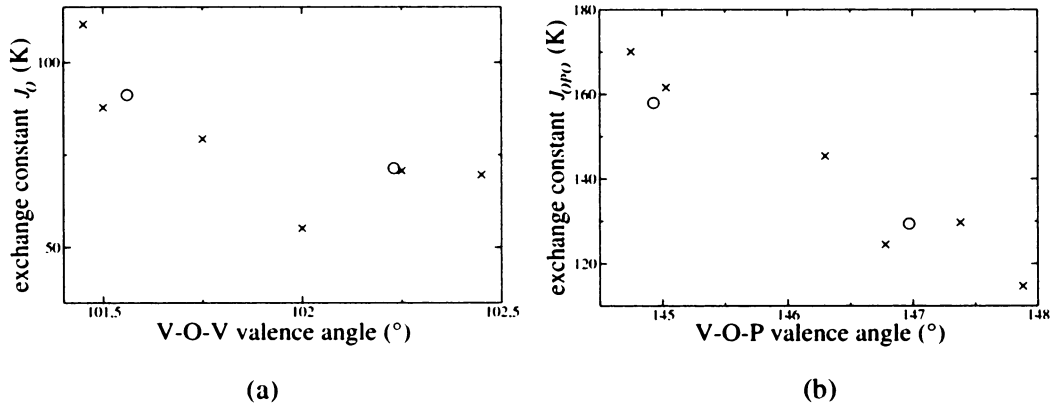

Figure 7. Exchange constant variations: (a) in D_O dimers as a function of the V−O−V angle and (b) in D_{OPO} dimers as a function of the V−O−P angle. The circles indicate the values calculated in the present paper; other points are taken from ref 21.

Table 3. Calculated Intrachain and Interchain Exchange Constant Parameters in the APO Phase[23]

	$J_{intrachain}$ (K)		$J_{interchain}$ (K)		$J_{interchain}$ (K)
D_O^A	71	O_1^A	−21	D_{OPO}^{C1}	−13
D_O^B	91	O_2^A	−33	D_{OPO}^{C2}	−13
D_{OPO}^A	129	O_1^B	−21	D_{OPO}^{C1}	−14
D_{OPO}^B	158	O_2^B	−32	D_{OPO}^{C1}	−12

Table 4. *Ab Initio* Values of the Hyperfine Constants (MHz) in the APO Phase[23]

phosphorus atom	*A* (MHz)
P1	4.00, 19.3, 28.2, 32.6
P2	13.7, 18.6, 27.2, 32.4
P3	13.9, 14.1, 28.1, 39.1
P4	16.4, 18.1, 30.8, 34.3

Let us examine similar simulations for the APO phase reported by Hiroi et al.[34] (Figure 6b). It is seen that the four signals are roughly split into three groups consisting of successively 1, 1, and 2 signals. The splitting inside the third group is approximately 3% of the maximum chemical shift. Therefore, the experimental deconvolution should exhibit only three different distinct signals with relative intensities 1:1:2, which are not actually observed. Moreover, in contrast with the experimental data, the lower signal turns out to be much smaller (∼4000 ppm) than the other ones.

These observations on the APO and APM phases strongly suggest that the experimental ^{31}P NMR data may have been reported on a monoclinic sample rather than on an orthorhombic[34] one.

However, two single-crystal X-ray structures of $(VO)_2P_2O_7$ have been recently determined with high precision.[23,35] From these resolutions, the space group is orthorhombic in both cases and the average structures are very similar to Hiroi's one (Figure 1). Extended Hückel calculations have shown that the exchange constant values are almost identical from one structure to the other. Therefore, we focused on one of these two systems, namely the structure reported by Koo et al.[23] A very similar strategy was used to simulate the NMR spectra from *ab initio* calculations of the magnetic exchange and hyperfine constants. Since *ab initio* exchange constant values have not been reported, we first looked into the different magnetic patterns. Based on the combined B3LYP-broken symmetry approach which has been recently suggested,[21,22] exchange constants were calculated and are reported in Table 3 for intrachain and interchain dimers.

As in our previous work on the APM and APO (Hiroi et al.[34]) phases, the dominant exchange constants are associated with the intrachain dimers. The interchain ferromagnetic interaction along the vanadyl bonds cannot be neglected (∼ −30 K), whereas the interchain interactions along the **c** direction are roughly −13 K. Thus, the magnetic interactions are suggestive of the model used for the APO (Hiroi et al.[34]) phase.

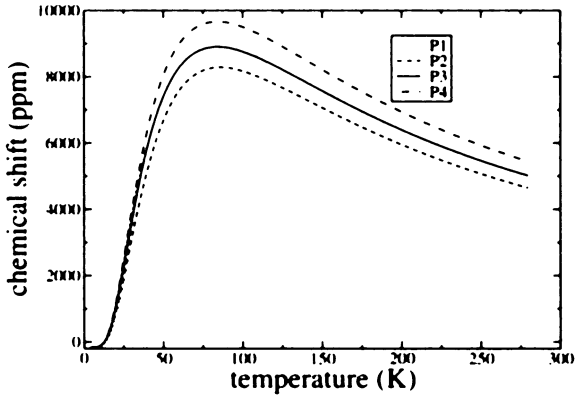

Figure 8. Temperature-dependent ^{31}P NMR simulation for the APO phase.[23]

Since, magneto-structural correlations have been previously reported for the D_O and D_{OPO} dimers, we examined the exchange constant variations with respect to the same angular parameters. As an interesting conclusion, the general trend in these correlations is observed (Figure 7a and b). Hyperfine constant calculations are reported in Table 4.

Based on these *ab initio* values, we performed temperature-dependent NMR signals for the APO phase (see Figure 8). One sees immediately that the four signals are split by approximately 10% of the maximum chemical shift. The experimental resolution being of the order of 15%, we may expect four separated signals, as it is actually observed. The agreement between experimental data and our simulations may support the presence of the newly synthesized APO phase in the studied sample. However, one should remember that the relative intensities are 1:3:3:1 in the NMR experiment, still suggesting the presence of eight nonequivalent phosphorus atoms.

3.3. Fit of ^{31}P NMR Experiments. In this section, our goal is to extract hyperfine coupling constants by fitting the

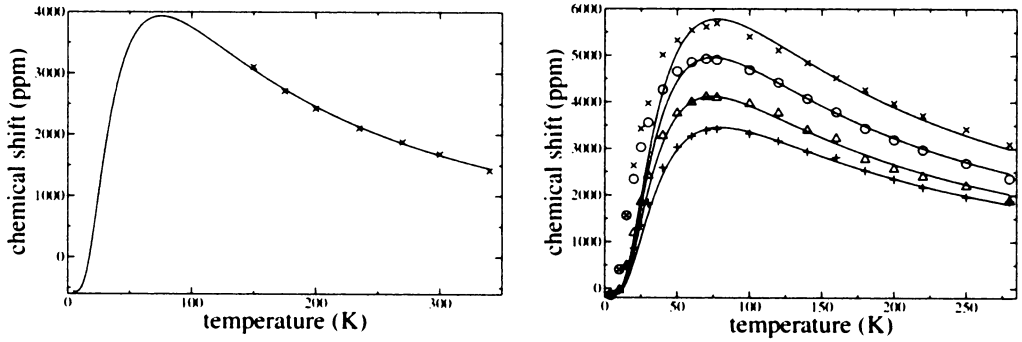

Figure 9. Adjustment of the ^{31}P NMR data (a) for the hemihydrate phase and (b) for the APM-$(VO)_2P_2O_7$.

Table 5. Extracted Values of the Hyperfine Constants (MHz) in the APM Phase

phosphorus atom	*A* (MHz)
P1	0.0, 5.0, 24.4, 24.6
P2	0.0, 0.0, 0.8, 43.7
P6	0.0, 0.0, 0.0, 36.8
P8	0.0, 5.1, 10.4, 18.1

experimental temperature-dependent NMR signals for the hemihydrate $VO(HPO_4)\cdot 0.5H_2O$ phase and the AP-$(VO)_2P_2O_7$ phase. Such an approach requires the knowledge of the local paramagnetic environment of each resonant phosphorus.

In the hemihydrate phase, the vanadium atoms are all equivalent, leading to a single F^{hemi} function. As mentioned in section 2.3, the paramagnetic part of the chemical shift depends on the sum of the two hyperfine constants A_{OPO} and A_{O}. The situation is slightly more difficult for the AP-$(VO)_2P_2O_7$ phase, since the nature of the sample is questionable. However, based on our *ab initio* spectra analysis, the APM phase turns out to be a good candidate. Since only four signals are experimentally observed, four phosphorus atoms had to be selected among the eight nonequivalent ones. Again, our *ab initio* simulations were very helpful in this attribution, as the eight signals can be gathered into four groups. The smallest and highest experimental temperature-dependent signals are associated to P1 and P8 (see Figure 6a), respectively. The other two signals can be arbitrarily attributed to P2 and P5. P3, P4 and P6, P7 give rise to indistinguishable signals to P2 and P5.

For the hemihydrate phase, the fit allows us to extract a diamagnetic part (−552 ppm) and the sum of the two hyperfine constants (40.7 MHz) with an *R*-factor $\approx 4 \times 10^{-5}$. For this phase, an underestimation of our *ab initio* calculations (17 MHz) reported in section 3.1 is observed. On the other hand, the diamagnetic part, or more exactly temperature-independent part of the paramagnetic shift, is clearly overestimated, probably due to a limited temperature range for our fit (150−340 K[30]). However, the nonmonotonic extrapolated curves (Figure 9a) peak near 70 K as compared to 60 K in the NMR experimental data.[31] For the APM phase, the hyperfine constants are reported in Table 5. The diamagnetic shift value is −130 ppm, and the *R*-factor $\approx 3 \times 10^{-4}$. The curves obtained with fitted parameters are shown in Figure 9b. The extracted hyperfine constants are roughly 1.5 times smaller than our *ab initio* calculations. However, the fitted constants are of the same order of magnitude as the previously reported values. Contrary to the fit of magnetic susceptibility, corrections due to paramagnetic impurities have not been performed on the NMR data. Thus, the relative disagreement on low temperature between the adjustment and the experimental data can be understood. Even though this scaling factor requires further investigations, the *ab initio* strategy has clarified the nature of the crystallographic phase by comparison of the experimental temperature-dependent NMR shifts and our simulations. In this respect, the latter was used as a guide in the attribution of the experimental NMR lines.

4. Conclusion

On the basis of *ab initio* exchange and hyperfine constants, we have reported original simulations of paramagnetic NMR spectra. To our knowledge, it is the first time such an *ab initio* approach has been used for the simulation of paramagnetic NMR spectra. The intriguing issue with respect to the number of signals has been debated for the APO and APM phases. The comparison to experimental data suggests that the sample which has been used in the NMR experiments may be monoclinic. Indeed, the eight simulated signals can be gathered into four groups with the relative ratio 1:3:3:1. This observation is consistent with the experimental signal intensities. For the recently synthesized orthorhombic phase, we have performed *ab initio* calculations of exchange and hyperfine constants. Despite the apparent disagreement in the relative intensities, the NMR simulated spectrum is very similar to the experimental one.

In that sense, we believe that further studies of ^{31}P NMR would be extremely valuable to support our conclusion in favor of the APM phase.

From the full *ab initio* simulations, we were able to identify the resonant phosphorus in the APM crystal structure. Based on this crucial information, the fit of NMR signals has led to the estimation of the diamagnetic part δ_{dia} and hyperfine constants.

In conclusion, the complementary approach between *ab initio* calculated exchange and hyperfine parameters and experimental fits turned out to be extremely powerful in the analysis of NMR paramagnetic shifts.

Acknowledgment. We are grateful to A. Tuel and J. Kikuchi for providing us with the experimental NMR data for $VO(HPO_4)\cdot 0.5H_2O$ and $(VO)_2P_2O_7$ compounds, respectively. The authors would like to thank F. H. Köhler for stimulating discussions upon NMR spectroscopy.

Supporting Information Available: One table showing the *ab initio* hyperfine constant values for the four phosphorus atoms of a chosen mononuclear complex. This material is available free of charge via the Internet at http://pubs.acs.org.

JA0292602